Eur. Radiol. (2001) 11: 559–566

Marco Zanetti
Thorsten Carstensen
Dominik Weishaupt
Bernhard Jost
Juerg Hodler

MR arthrographic variability of the arthroscopically normal glenoid labrum: qualitative and quantitative assessment

Received: 29 November 1999
Revised: 10 May 2000
Accepted: 23 August 2000

M. Zanetti (✉) · T. Carstensen ·
D. Weishaupt · J. Hodler
Department of Radiology,
University Hospital Balgrist,
Forchstrasse 340, 8008 Zurich, Switzerland
e-mail: mzanetti@balgrist.unizh.ch
Tel.: + 41-1-386 33 03
Fax: + 41-1-386 33 19

B. Jost
Department of Orthopedic Surgery,
University Hospital Balgrist,
Forchstrasse 340, 8008 Zurich, Switzerland

Abstract The purpose of this study was to assess qualitatively and quantitatively the MR arthrographic variability of the arthroscopically normal glenoid labrum. Form and signal abnormalities of arthroscopically normal labral parts were analyzed on axial and coronal MR arthrograms of 55 consecutive patients (mean age 43.8 years, age range 21–76 years) referred mainly for suspected rotator cuff lesions. Length and width of the labrum were measured. One hundred twenty-one of 241 (50 %) arthroscopically normal labral parts demonstrated normal (low) signal intensity and normal form on MR arthrograms. Increased linear or globular signal intensity was present in 74 of 241 (31 %) normal labral parts, deformed or fragmented labra in 28 (12 %), complete separation of the labrum from the glenoid in 4 (2 %), a cleft in 5 (2 %), attenuation in 4 (2 %), and complete absence in 5 (2 %), respectively. The mean size of the normal labrum varied between 3.8 × 3.3 mm at the subscapularis bursa level (anteriorly) and 6.1 × 5.6 mm at the inferior portion of the glenoid (anteriorly). The size was not significantly different between arthroscopically normal and abnormal labral parts (p = 0.13–0.83). Since the MR appearance of the arthroscopically normal glenoid labrum varies considerably concerning signal intensity, form, and size, only major tears or detachments of the labrum should be diagnosed.

Key words Shoulder · MR imaging · MR arthrography · Shoulder anatomy · Glenoid labrum

Introduction

The glenoid labrum is a fibro-cartilaginous structure that is firmly attached to the glenoid rim inferiorly and posteriorly, thereby adding depth and contributing to the stability of the joint [1]. The superior part of the labrum tends to be meniscus-like, more loosely attached, and more mobile. On MR images, the normal labrum is usually triangular in the anterior and superior portions and rounded in the posterior and inferior portions [1]. However, the appearance of the labrum on standard MR images is highly variable in asymptomatic persons as demonstrated previously [2, 3, 4, 5]. This may lead to considerable diagnostic difficulty [2, 4]. Foreshortening and thinning of the labrum have been suggested as signs of abnormality [1]. However, such diagnosis may be difficult in a specific situation because, to our knowledge, no information is available about the size of the normal labrum at various levels. Compared with standard MR imaging, MR arthrography affords better visualization of the labral shape and labral detachment [6].

The superior glenoid labrum has received special attention in the literature due to the so-called lesion of the superior glenoid labrum with anterior to posterior extension (SLAP lesion) [7, 8, 9]. For this clinically important diagnosis MR imaging has been employed [9, 10]. Diagnostic problems occur in the presence of a su-

blabral recess in patients without any evidence of trauma. Such recesses are common in the anterior part of the superior labrum [8, 11, 12].

We investigated qualitatively and quantitatively the MR arthrographic appearance of arthroscopically normal labral parts. Specifically, we evaluated the significance of signal and form abnormalities which previously have been associated with labrum abnormality [4, 8, 13, 14, 15, 16].

Materials and methods

Based on a surgical record data base of 180 patients, 55 patients were included consecutively in this retrospective investigation between January 1996 and January 1998 when they had at least one arthroscopically normal part of the labrum. All MR arthrograms had to be performed at our institution according to a standardized imaging protocol. The time delay between MR arthrography and arthroscopy was no longer than 3 months. The main indications for MR arthrography were suspected rotator cuff abnormalities (33 patients), biceps tendon abnormalities (10 patients), chronic unexplained shoulder pain (8 patients), and instability (4 patients). The scarcity of unstable shoulders is explained by the fact that CT arthrography is preferred by our shoulder surgeons in instability patients because glenoid rim fractures are more conspicuous on CT compared with MR imaging [17]. Arthroscopy was performed by an experienced orthopedic shoulder surgeon. The resulting group consisted of 34 men and 21 women, with a mean age of 43.8 years (age range of 21–76 years). Any abnormal parts of the labrum described by the orthopedic surgeons as degenerative, synovitic, hypermobile, detached or thickened were included as controls. Labral regions not specifically described by the orthopedic surgeons were not further evaluated.

MR imaging

Magnetic resonance imaging was performed on a 1.0-T scanner (Siemens Impact-Expert, Siemens, Erlangen, Germany). The shoulder was placed in a dedicated receive-only shoulder coil. All patients had an MR arthrographic examination after intra-articular injection of 10–15 ml diluted gadopentetate (4 mmol/l) according to our institution's standardized imaging protocols. The joint was punctured under fluoroscopic guidance. Intra-articular position of the needle tip was confirmed by injection of 1 ml Iopamidol 408 (Iopamiro, Bracco, Milan, Italy). Informed consent was obtained from the patients for MR arthrography. This method was also approved by the hospital's ethics committee and the responsible state agency. Coronal oblique and axial images were obtained. Three-dimensional fast imaging with steady-state precession (FISP) images were obtained in the coronal oblique and axial planes. Coronal oblique sequences were planned perpendicular to the glenohumeral joint. Repetition time (TR) was 32 ms, echo time (TE) 10 ms, and flip angle 40°. A 50-mm slab of 16 of slices was obtained resulting in a slice thickness of 3.1 mm. The field of view was 160 or 180 mm. Image matrix was 192 × 256, the number of acquisition was one, and imaging time was 1 h 40 min. In the coronal oblique plane, proton-density weighted and T2-weighted turbo spin-echo (TSE) images were also obtained (TR 3500 ms, TE 15/105 ms, number of echoes 2, echo train length 7, slice thickness 3.0 mm, field of view 160 or 180 mm, image matrix of 192 × 256, 4 acquisitions, and imaging time of 3 h 52 min to 4 h 48 min).

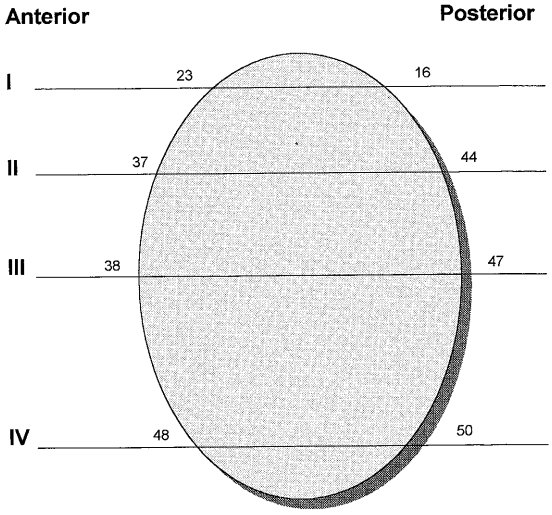

Fig. 1 The glenoid surface depicts the four levels (I–IV) used in this investigation and denotes the number of individual labral parts that were analyzed. *I* superior glenoid level; *II* bursa subscapularis level; *III* mid-glenoid level; *IV* inferior glenoid level

Image analysis

Each of the imaging sequences were evaluated by two experienced musculoskeletal radiologists without knowledge of the arthroscopy reports. Evaluation was performed by consensus reading. Both musculoskeletal radiologists were different from the person who gathered the cases.

Both qualitative and quantitative assessment of the labrum was performed at each of four levels for each of the anterior and posterior labrum giving a total of eight labral parts. The four levels (Fig. 1) were defined according to Zlatkin et al. [18]: level 1 = superior portion of the glenoid (one section lower than the origin of the biceps tendon); level 2 = subscapularis bursa; level 3 = mid-glenoid level; and level 4 = inferior glenoid.

Form and signal abnormalities of the anterior and posterior labrum were analyzed in the axial plane using the classification published by McCauley et al. [4]: 0 = normal, uniform low signal intensity compared with muscle with a triangular or round configuration of the labrum (Fig. 2); I = linear high signal intensity at the junction of the labrum and glenoid; II = linear or globular high signal intensity in the labrum (Figs. 3, 5); III = linear high signal intensity extending through the labrum to both surfaces; IV = cleft in the labrum (Fig. 4); V = separation of the labrum from the surface of the glenoid cavity (Figs. 3, 5); VI = deformed labrum (irregular contours or fragmented; Fig. 5); VII = attenuation (marked reduction in size; Fig. 6); and VIII = absent labrum.

At each location the length of the labrum was measured parallel to the glenoid rim and the width of the labrum perpendicular to the glenoid (1 and 2, respectively, in Fig. 2).

The biceps anchor/superior labrum complex was evaluated on the coronal oblique sequence with regard to length and width, location, and appearance of any recess-like signal abnormalities at the labral base [which may mimic a superior labral tear oriented in the anterior to posterior direction (SLAP lesion)]. This recess was classified as 0 = none; 1 = smooth recess (Fig. 6); 2 = recess with irregular contours; and 3 = recess with an additional cleft (Fig. 7). The length (cranial–caudal direction) and the width of the recess were measured (Fig. 7b). The extent of the recess in the anteri-

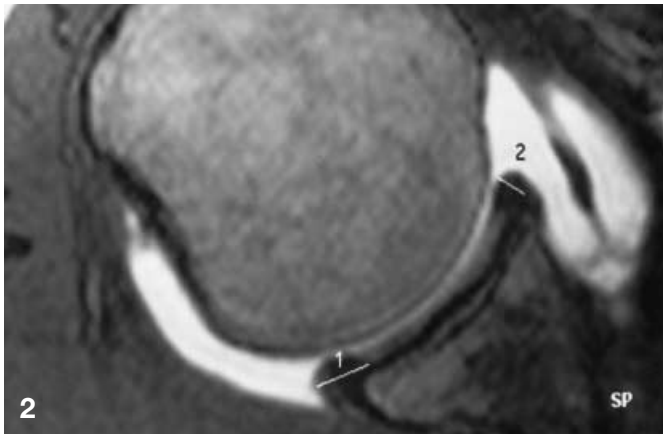

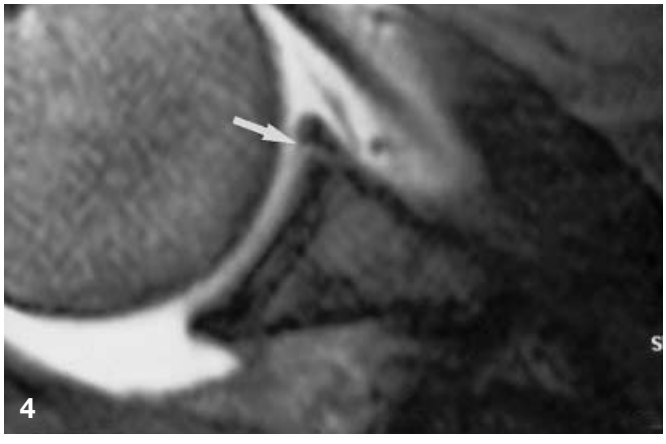

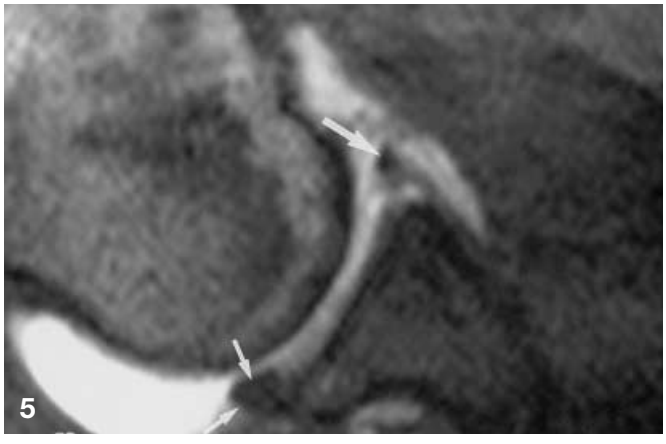

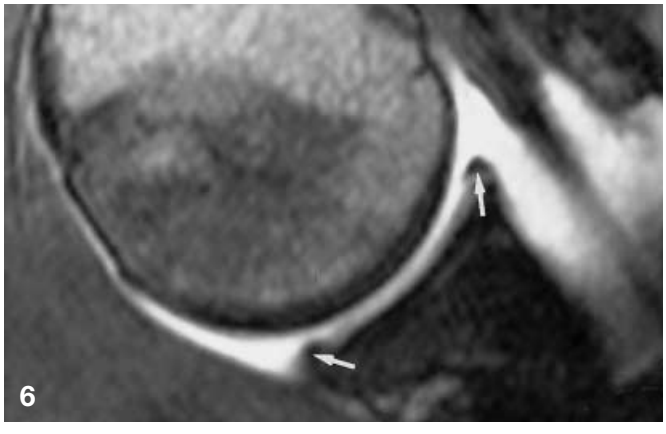

Fig. 2 A 49-year-old man with impingement syndrome. Measurement of normal anterior and posterior labrum on an axial 3D fast imaging with steady-state precession (FISP) image (TR 32 ms, TE 10 ms, flip angle 40°). The length and width of the labrum were measured parallel *(1)* and perpendicular *(2)* to the glenoid, respectively

Fig. 3 A 22-year-old woman with anterior instability and arthroscopically proven detachment of the anterior labrum. Slightly increased signal in the posterior labrum (type II; *small arrows*) and separation of the anterior labrum (*arrow*; type V). Axial 3D FISP image (TR 32 ms, TE 10 ms, flip angle 40°) at the level of the subscapularis bursa

Fig. 4 A 53-year-old woman with rotator cuff rupture. Normal labrum at arthroscopy. Cleft in the labrum (*arrow*; type IV). Axial 3D FISP MR image (TR 32 ms/TE 10 ms/flip angle 40°) at the mid glenoid level. The posterior labrum was considered to be normal

Fig. 5 A 22-year-old woman with anterior instability, anterior labrum detached, same patient as in Fig. 3. Axial 3D FISP MR image (TR 32 ms/TE 10 ms/flip angle 40°) at the mid glenoid level. Globular signal in the posterior labrum (*small arrows*; type II) and deformed anterior labrum with irregular contours (*large arrow*; type VI)

Fig. 6 A 23-year-old man with partial rupture of the biceps tendon. Labrum arthroscopically normal. Attenuation of the anterior and posterior labrum (*arrows*; type VII). A small cleft anteriorly is also visible. Axial 3D FISP MR image (TR 32 ms/TE 10 ms/flip angle 40°) at the level of the subscapularis bursa

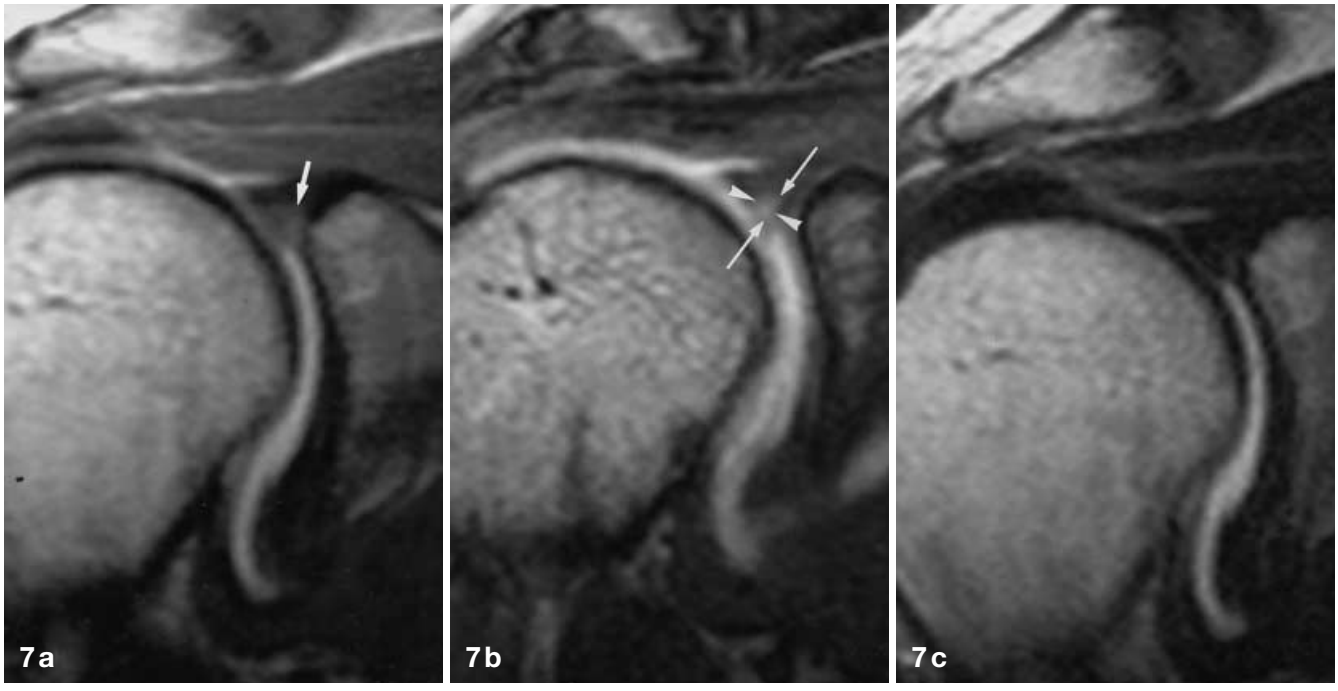

Fig. 7a–c A 55-year-old man with a partial tear of the supraspinatus tendon. Recess-like signal abnormality in an arthroscopically normal biceps anchor. **a** Coronal oblique proton-density-weighted MR image (TR 3500 ms, TE 15 ms) and **b** 3D FISP MR image (TR 32 ms/TE 10 ms/flip angle 40°) demonstrate recess-like signal abnormality at the labral base (*arrows*, *arrowheads*). The signal abnormalities are more conspicuous than on the proton-density-weighted MR image. Moreover, the recess-like signal abnormality appears larger. The length of the recess was measured between the arrows and the width between the *arrowheads*, respectively. **c** On the corresponding T2-weighted (TR 3500 ms, TE 105 ms) MR image a recess was not diagnosed prospectively by the readers

Fig. 8 A 40-year-old man in whom a detached biceps anchor (SLAP II) was found at arthroscopy. Coronal 3D FISP MR image (TR 32 ms/TE 10 ms/flip angle 40°) demonstrates recess-like signal abnormality *(thick arrow)* adjacent to the glenoid and an additional cleft *(thin arrow)*

or–posterior direction was classified as follows: (a) anterior to the biceps tendon; (b) extension from anteriorly into the biceps anchor; and (c) extension from anterior throughout the biceps anchor to the labrum posterior to the biceps tendon.

For comparison of the form and the size in normal and abnormal labral parts, unpaired two-tailed *t*-tests were used for continuous numbers, analysis of variance for nominal categories. The *p*-values of 0.05 and lower were considered to represent statistical significance.

Results

Of the 440 theoretically available labral parts, 361 were described during arthroscopy. Of these 361 labral parts, 283 were normal and 78 abnormal. Of the 361 labral parts, 303 could be identified on MR arthrograms and were further evaluated. The 58 remaining labral parts were not included due to inadequate image quality

Table 1 MR arthrographic findings on axial 3D gradient echo MR images in normal and abnormal labra

MR arthrography		Arthroscopy			
		Anterior labrum		Posterior labrum	
Grade	Description	Normal[a]	Abnormal[b]	Normal[c]	Abnormal[d]
0	Normal signal intensity and configuration	42 (36)	15 (41)	79 (64)	9 (36)
I	Linear high signal intensity at the junction of the labrum	0 (0)	0 (0)	0 (0)	1 (4)
II	Linear or globular high signal intensity in the labrum	37 (31)	13 (35)	37 (30)	8 (32)
III	Linear high signal intensity extending to both surfaces	0 (0)	0 (0)	0 (0)	0 (0)
IV	Cleft in the labrum	5 (4)	0 (0)	0 (0)	1 (4)
V	Separation of the labrum	3 (3)	2 (5)	1 (1)	2 (8)
VI	Deformed labrum with irregular contours or fragmented	24 (20)	6 (16)	4 (3)	4 (16)
VII	Marked reduction in size (attenuated)	2 (2)	0 (0)	2 (2)	0 (0)
VIII	Absent labrum	5 (4)	1 (3)	0 (0)	0 (0)
Total		118 (100)	37 (100)	123 (100)	25 (100)

Numbers in parentheses are percentages
[a]Percentage of all normal anterior labra
[b]Percentage of all abnormal anterior labra
[c]Percentage of all normal posterior labra
[d]Percentage of all abnormal posterior labra

Table 2 Quantitative assessment of the normal labrum on axial 3D gradient-echo MR images

Location	Normal labral parts ($n = 241$)				Significance *(p)*	
	Anterior (mm)		Posterior (mm)		Anterior	Posterior
	Length (SD)	Width (SD)	Length (SD)	Width (SD)	Length/width	Length/width
Superior glenoid	4.3 (0.34)	3.7 (0.34)	5.3 (0.57)	4.3 (0.46)	0.64/0.80	0.57/0.80
Subscapularis bursa	3.8 (0.33)	3.3 (0.27)	4.5 (0.31)	3.6 (0.23)	0.48/0.83	0.54/0.31
Mid-glenoid	5.3 (0.33)	4.6 (0.34)	4.9 (0.28)	3.7 (0.26)	0.86/0.77	0.21/0.25
Inferior glenoid	6.1 (0.43)	5.6 (0.41)	5.8 (0.33)	4.4 (0.25)	0.19/0.13	0.14/0.71

Significance values for Student's *t*-test for differences between arthroscopically normal and abnormal labral parts

(para-articular contrast, insufficient delineation by contrast medium, and/or motion artifacts). There remained 241 arthroscopically normal and 62 abnormal labral parts in the investigation. At arthroscopy the 62 abnormal labral parts were characterized as degenerative ($n = 31$), synovitic ($n = 5$), hypermobile ($n = 5$), detached ($n = 14$), or thickened ($n = 7$). One anterior–superior sublabral foramen was found at arthroscopy. A Buford Complex was not described in this series.

Normal labrum

One hundred twenty-one of 241 (50 %) arthroscopically normal labral parts demonstrated normal (low) signal intensity and normal form on MR arthrograms. Increased linear or globular high signal intensity of the labrum was present in 74 of 241 (31 %) arthroscopically normal labral parts, deformation with irregular contours or fragmentation in 28 (12 %), complete separation of the labrum in 4 (2 %), a cleft in 5 (2 %), attenuation (marked reduction in size) in 4 (2 %), and complete absence in 5 (2 %), respectively. Linear signal at the labral base (type I) or extending to both surfaces (type III) were not diagnosed. The detailed results separated for the anterior and posterior labrum assessed on the 3D FISP axial sequence are demonstrated in Table 1.

The mean size of the normal labrum varied between 3.8 × 3.3 mm at the subscapularis bursa level (anteriorly) and 6.1 × 5.6 mm at the inferior portion of the glenoid (anteriorly) (Table 2).

Comparison of the normal and abnormal labrum

Analysis of variance regions did not show any significant difference between normal and abnormal labral parts when applied to qualitative MR grading (grades I–VIII). The *p*-values at level 1 were 0.25 anteriorly and 0.09 posteriorly; 0.10/0.13 at level 2; 0.07/0.15 at level 3, and 0.82/0.66 at level 4, respectively.

The mean diameters of the normal and abnormal labrum was not significantly different ($p = 0.13$–0.83; Table 2).

Biceps anchor

The biceps anchor was described in 54 of 55 arthroscopic reports. In 30 patients the biceps anchor was

Table 3 Recess-like abnormalities in normal and abnormal biceps anchors on coronal oblique MR images. *FISP* 3D fast imaging with steady-state precession (gradient-echo sequence)

MR arthrographic findings		Normal anchor (n = 30)			Abnormal anchor (n = 24)		
		Proton density	T2-weighted	FISP	Proton density	T2-weighted	FISP
Form	None	20	27	19	12	15	12
	Smooth	9	3	10	10	7	8
	Irregular contours	1	0	1	0	0	1
	Additional cleft	0	0	0	2	2	3
p		0.15	0.042	0.15			
Extension	None	20	27	19	12	15	12
	Anterior to biceps tendon	4	3	4	3	1	2
	At biceps anchor	2	0	1	0	0	1
	Posterior to biceps tendon	4	0	6	9	8	9
p		0.10	0.0006	0.53			

p-value for likelihood ratios for analysis of variance for nominal categories between arthroscopically normal and abnormal biceps anchor

Table 4 Mean size and SD of recess-like abnormalities in normal and abnormal biceps anchors on coronal oblique proton-density turbo spin-echo and 3D FISP MR images. *FISP* 3D fast imaging with steady-state precession (gradient-echo sequence)

		Arthroscopically Normal biceps anchor (n = 30)			Arthroscopically Abnormal biceps anchor (n = 24)		
		No. of recesses	Length (SD)	Width (SD)	No. of recesses	Length (SD)	Width (SD)
Proton-density turbo	Spin-echo sequence	10	1.1 (0.35)	0.7 (0.20)	12	1.8 (0.39)	1.0 (0.23)
p			0.20	0.47			
FISP		11	3.2 (0.48)	2.1 (0.16)	12	3.3 (0.51)	1.9 (0.15)
p			0.91	0.34			

Significance *(p)* for difference of the size of the recess-like abnormalities in normal and abnormal biceps anchors (unpaired t-test)

normal. There was a SLAP-I lesion (marked fraying with degenerative appearance of the superior labrum, but peripheral labral edge remained firmly attached to the glenoid) in 17 patients, a SLAP-II lesion (superior labrum and attached biceps tendon stripped off the underlying glenoid) in 6, and a SLAP-III lesion (bucket-handle tear in the superior labrum) in 1 patient, respectively. A SLAP-IV lesion (bucket-handle tear in the superior labrum with extension in the biceps tendon) was not identified in this study.

Normal biceps anchor

In 30 arthroscopically normal biceps anchors recess-like increased signal was found at the base of the labrum on 3 (10%) T2-weighted MR arthrograms, on 9 (30%) proton-density MR arthrograms and on 10 (33%) FISP MR arthrograms (Table 3). An irregular recess-like signal abnormality in an arthroscopically normal biceps anchor was found in one proton-density and one FISP MR image each. An additional cleft was never found in arthroscopically normal biceps anchors. The mean size of the recess-like signal abnormality was larger on FISP MR images (length 3.3 mm, width 1.1 mm) compared with the size measured on proton-density-weighted MR images (1.0 and 0.7 mm, respectively; Fig. 7; Table 4).

Comparison of normal and abnormal biceps anchor

A significant difference was found on T2-weighted MR images with regard to the form of the recess-like signal abnormality (none, smooth, irregular, additional cleft; $p = 0.042$) and extension posterior to the biceps anchor (type C) ($p = 0.0006$; Table 3).

Discussion

Variability of the normal glenoid labrum

The arthroscopically normal labrum is very variable and the reliability of several previously published MR signs in diagnosing labral abnormalities can be questioned. In our series only 50% of the arthroscopically normal labral parts were completely unremarkable on MR arthrograms. On the other hand, complete detachment,

clefts, and complete absence of the labrum were rare in the arthroscopically normal labrum. However, analysis of variance regions did not show any significant difference between normal and abnormal labral parts when applied to qualitative MR grading (grades I–VIII). Quantitative analysis of labral size also revealed a large variability among arthroscopically normal labral parts. A statistically significant difference between normal and abnormal labral parts was not found; therefore, the value of size criteria is limited. Admittedly, our control group in patients predominantly suffering from rotator cuff abnormalities consisted of only minor labral abnormalities such as degeneration, thickening, or synovitic changes. Moreover, our standard of reference has potential limitations: Arthroscopy was not performed prospectively for labrum abnormalities, and labral findings might have been missed. The retrospective study design may also explain some of the discrepancies between surgery and imaging produced by problems of spatial correlation of imaging and arthroscopy findings. Nevertheless, the results of our study are in accordance with a previous publication using CT arthrograms [19]. McNiesh and Callaghan [19] reported a notched, cleaved, or small anterior labrum occurring as a normal variation. The variability of the labral shape has also been demonstrated on standard MR images in asymptomatic persons [20] and arthroscopically normal labra [21]. Neuman and coworkers [20] demonstrated labral variations as follows: the anterior part of the labrum was triangular (45 %), round (19 %), cleaved (15 %), notched (8 %), flat (7 %), or absent (6 %); and the posterior labrum was triangular (73 %), round (12 %), flat (6 %), or absent (8 %). These findings are also compatible with our findings which indicate higher variability of the anterior than the posterior labrum (Table 1). Tuite and Orwin [5] reported a relatively low specificity (0.54–0.64) in the evaluation of the labrum with standard MR images and emphasized that one of the reasons was increased signal in arthroscopically normal labra.

Despite the variability of the labrum on MR images in asymptomatic or arthroscopically normal joints, high accuracy of cross-sectional imaging methods has been reported for labral abnormalities [13, 14, 22]. Deutsch and colleagues [22] were able to characterize accurately the glenoid labrum in 38 patients (sensitivity 96 %, accuracy 86 %) in an investigation of 44 patients using computed arthrotomography and surgical correlation. Legan and coworkers [13] reported that standard MR imaging had a sensitivity of 95 % and a specificity of 86 % for anterior labral tears. An even higher specificity (93 %) and a similarly high sensitivity (91 %) has been reported for MR arthrography [14]. However, although our investigation may be biased against imaging due the presence of only minor degenerative abnormalities in a middle-aged population, these studies may be biased in favor of imaging due to the high prevalence of large labral abnormalities in predominantly young men with athletic injuries. The importance of the patient population who requires MR imaging for labral abnormalities has recently been emphasized by another group [23]: In middle-aged patients (mean age 40 years) with chronic glenohumeral joint instability MR arthrography had a lower sensitivity (80 %) and specificity (81 %) in the diagnosis of labral tears than prior reports which have included patients with acute injuries [13]. They explained this result by attempted healing that takes place from the time of injury to the time of imaging which may obscure the underlying injury. Moreover, signal abnormalities may become more common with normal aging due to mucinous and myxoid changes of the labral substance [24]. Such degeneration may not be visible during arthroscopy or surgery but produces increased signal on MR images. In addition, the gradient-echo sequence employed in our investigation may increase the prevalence of signal abnormalities if compared with standard spin-echo images.

We are also aware that arthroscopically normal labral parts may be abnormal histologically; however, such abnormalities are not relevant for surgical decision making and were not evaluated in this investigation.

Recess-like signal abnormalities at the biceps anchor

Recess-like abnormalities were commonly found on MR arthrograms of arthroscopically normal biceps anchors. This is not unanticipated considering that in a previously published cadaver study such a recess was present in 19 of 26 (73 %) shoulders [8]. It had an appearance similar to that of published examples of SLAP lesions. Histologically, there was no evidence of fibrosis suggesting a traumatic cause in this investigation. Another group found a similar frequency of sublabral recesses (12 of 17 = 71 %) in cadavers. All recesses were covered by two or three layers of synoviocytes [12]. The frequent presence of sublabral recesses in these cadaver studies is consistent with the experience of our orthopedic surgeons that a small recess is frequently found in portions of the biceps anchor. In such cases the biceps anchor is classified as normal when the anchor is stable during testing with a hook. In our study, we found recess-like abnormalities in arthroscopically normal labral parts most commonly on gradient-echo images (in 33 % of the normal anchors) which apparently overestimates alterations of the labral base. The lower value of gradient-echo MR images in labrum evaluation has previously been demonstrated by McCauley et al. [4]. They concluded that increased intralabral signal intensity on gradient-echo images does not predict labral integrity. Such an overestimation of labrum abnormality is probably also responsible for the apparently larger size of

the recess on gradient-echo MR images compared with proton-density-weighted images. On T2-weighted images these signal abnormalities were less frequently seen. When signal abnormalities at the biceps anchor were visible on T2-weighted images and when they extended posterior to the biceps anchor, a high association with surgical abnormality was found ($p = 0.0006$). This is also in accordance with Smith and coworkers who suggested that a SLAP lesion should be considered if the recess extends posterior to the biceps anchor [8]. An additional cleft visible in the biceps anchors appears to be a sign for SLAP lesion because we have never found such a finding in normal biceps anchors.

In conclusion, MR arthrography may be less useful in the preoperative evaluation of the glenoid labrum than previously thought, because the MR appearance of the arthroscopically normal glenoid labrum varies considerably concerning signal intensity, form, and size. Only major tears or detachments of the labrum should be diagnosed on MR arthrograms, especially in middle-aged patients.

References

1. Resnick D (1995) Arthrography, tenography, and bursography. In: Resnick D (ed) Diagnosis in bone and joint disorders, vol 1. Saunders, Philadelphia, pp 277–409
2. Chandnani V, Ho C, Gerharter J, Neumann C, Kursunoglu-Brahme S, Sartoris DJ, Resnick D (1992) MR findings in asymptomatic shoulders: a blind analysis using symptomatic shoulders as controls. Clin Imaging 16: 25–30
3. Kaplan PA, Bryans KC, Davick JP, Otte M, Stinson WW, Dussault RG (1992) MR imaging of the normal shoulder: variants and pitfalls. Radiology 184: 519–524
4. McCauley TR, Pope CF, Jokl P (1992) Normal and abnormal glenoid labrum: assessment with multiplanar gradient-echo MR imaging. Radiology 183: 35–37
5. Tuite MJ, Orwin JF (1996) Anterosuperior labral variants of the shoulder: appearance on gradient-recalled-echo and fast spin-echo MR images. Radiology 199: 537–540
6. Chandnani VP, Yeager TD, DeBerardino T, Christensen K, Gagliardi JA, Heitz DR, Baird DE, Hansen MF (1993) Glenoid labral tears: prospective evaluation with MRI imaging, MR arthrography, and CT arthrography. Am J Roentgenol 161: 1229–1235
7. Snyder SJ, Karzel RP, Del Pizzo W, Ferkel RD, Friedman MJ (1990) SLAP lesions of the shoulder. Arthroscopy 6: 274–279
8. Smith DK, Chopp TM, Aufdemorte TB, Witkowski EG, Jones RC (1996) Sublabral recess of the superior glenoid labrum: study of cadavers with conventional nonenhanced MR imaging, MR arthrography, anatomic dissection, and limited histologic examination. Radiology 201: 251–256
9. Monu JU, Pope TL, Chabon SJ, Vanarthos WJ (1994) MR diagnosis of superior labral anterior (SLAP) injuries of the glenoid labrum: value of routine imaging without intraarticular injection of contrast material. Am J Roentgenol 163: 1425–1429
10. Hodler J, Kursunoglu-Brahme S, Flannigan B, Snyder SJ, Karzel RP, Resnick D (1992) Injuries of the superior portion of the glenoid labrum involving the insertion of the biceps tendon: MR imaging findings in nine cases. Am J Roentgenol 159: 565–568
11. Kwak SM, Brown RR, Resnick D, Trudell D, Applegate GR, Haghighi P (1998) Anatomy, anatomic variations, and pathology of the 11- to 3-o'clock position of the glenoid labrum: findings on MR arthrography and anatomic sections. Am J Roentgenol 171: 235–238
12. Kreitner KF, Botchen K, Rude J, Bittinger F, Krummenauer F, Thelen M (1998) Superior labrum and labral–bicipital complex: MR imaging with pathologic–anatomic and histologic correlation. Am J Roentgenol 170: 599–605
13. Legan JM, Burkhard TK, Goff WB, Balsara ZN, Martinez AJ, Burks DD, Kallman DA, Lapoint JM (1991) Tears of the glenoid labrum: MR imaging of 88 arthroscopically confirmed cases. Radiology 179: 241–246
14. Palmer WE, Brown JH, Rosenthal DI (1994) Labral-ligamentous complex of the shoulder: evaluation with MR arthrography. Radiology 190: 645–651
15. Allmann KH, Walter O, Laubenberger J, Uhl M, Buitrago-Tellez CH, Biebow N, Langer M (1998) Magnetic resonance diagnosis of the anterior labrum and capsule. Effect of field strength on efficacy. Invest Radiol 33: 415–420
16. Blum A, Coudane H, Mole D (2000) Gleno-humeral instabilities. Eur Radiol 10: 63–82
17. Kreitner KF, Runkel M, Grebe P, Just M, Schweden F, Oberbillig C, Schwickert H, Kirschner P, Schild HH (1992) MR tomography versus CT arthrography in glenohumeral instabilities. Fortschr Roentgenstr 157: 37–42
18. Zlatkin MB, Bjorkengren AG, Gylys-Morin V, Resnick D, Sartoris DJ (1988) Cross-sectional imaging of the capsular mechanism of the glenohumeral joint. Am J Roentgenol 150: 151–158
19. McNiesh LM, Callaghan JJ (1987) CT arthrography of the shoulder: variations of the glenoid labrum. Am J Roentgenol 149: 963–966
20. Neumann CH, Petersen SA, Jahnke AH (1991) MR imaging of the labral-capsular complex: normal variations. Am J Roentgenol 157: 1015–1021
21. Tuite MJ, Shinners TJ, Hollister MC, Orwin JF (1999) Fat-suppressed fast spin-echo mid-TE (TE[effective] = 34) MR images: comparison with fast spin-echo T2-weighted images for the diagnosis of tears and anatomic variants of the glenoid labrum. Skeletal Radiol 28: 685–690
22. Deutsch AL, Resnick D, Mink JH, Berman JL, Cone ROd, Resnik CS, Danzig L, Guerra J Jr (1984) Computed and conventional arthrotomography of the glenohumeral joint: normal anatomy and clinical experience. Radiology 153: 603–609
23. Kwak SM, Applegate GR, Snyder SJ, Yeh L, Resnick DL (1998) Chronic glenohumeral joint instability: evaluation with MR arthrography and correlation with arthroscopy. Radiology 209 (Suppl):400
24. Loredo R, Longo C, Salonen D, Yu J, Haghighi P, Trudell D, Clopton P, Resnick D (1995) Glenoid labrum: MR imaging with histologic correlation. Radiology 196: 33–41